

Flame-spraying synthesis of aluminate glasses in the Al_2O_3 – La_2O_3 system

Anna Haliaková^{a,*}, Anna Prnová^a, Róbert Klement^a, Dušan Galusek^a, Wei-Hsing Tuan^b

^a *Vitrum Laugaricio – Joint Glass Centre of the IIC SAS, TnU AD, FChPT STU, and RONA, j.s.c., Študentská 2, 911 01 Trenčín, Slovak Republic*

^b *Materials Science & Engineering, National Taiwan University, Taipei, Taiwan*

Received 9 September 2011; received in revised form 26 March 2012; accepted 29 March 2012

Available online 5 April 2012

Abstract

The paper deals with the synthesis and characterisation of binary aluminate glasses in the La_2O_3 – Al_2O_3 system with Al_2O_3 contents changing between 74.6 and 86.9 mol% (48–65 wt.%), and of ternary glasses with 75.7 mol% Al_2O_3 doped with 1 mol% of Nd_2O_3 or Er_2O_3 . Six binary and two ternary compositions were prepared. Flame synthesis facilitated the preparation of X-ray amorphous microspheres in the systems with 58 wt.% Al_2O_3 , and with eutectic composition in the pseudobinary LaAlO_3 – $\text{LaAl}_{11}\text{O}_{18}$ system doped with Er. Other systems contained low fractions of crystalline LaAlO_3 perovskite, regardless of the composition. The diameter of prepared microspheres ranged between 2 and 10 μm . They were transparent for visible light, as well as in the IR wavenumber range from 1300 to 4000 cm^{-1} .

© 2012 Elsevier Ltd and Techna Group S.r.l. All rights reserved.

Keywords: Alumina; Rare earth oxides; Flame-spraying synthesis; Glass microspheres

1. Introduction

Aluminate glasses with high alumina contents are expected to exhibit outstanding mechanical and optical properties, especially hardness, high refraction index, transparency in IR region and high chemical resistance, which are comparable to single crystal sapphire [1]. However, the preparation of such glasses is usually difficult due to high melting temperatures, often approaching to 2000 °C, and high tendency to crystallization. High cooling rates up to 10³ K s^{−1} are, therefore, required for their successful preparation [2]. The preparation and structure of binary and ternary glasses with high alumina contents have been dealt with in several published works, and successful preparation of glasses in the Al_2O_3 –CaO [3], Al_2O_3 –SiO₂ [4], Al_2O_3 –Re₂O₃, where Re = La, Y, Yb, Nd [4,5] and Al_2O_3 –Re₂O₃ (Re = Y, La, Gd) systems [2] has been reported. The structure of Nd_2O_3 doped silica and La_2O_3 + Y_2O_3 + Al_2O_3 glasses was studied and described by Benmore et al. [6].

For the preparation of such glasses whole range of techniques were described in literature. Their common features are high melting temperatures and the possibility to achieve high cooling rates. Aronne et al. [7] prepared the lanthanum–aluminosilicate

glasses by melting the glass batch in a platinum crucible in an electrically heated furnace. The melt was quenched by immersing the crucible into cold water. Similar method could be also used for the preparation of lanthanum–aluminophosphate glasses [8], as well as for the ternary Re_2O_3 – Al_2O_3 glasses with 5–30 mol% SiO₂ addition [4], where the presence of SiO₂ and P₂O₅ enhances glass forming ability and stability of prepared glasses. More sophisticated methods with extremely high cooling rates are required especially in case of binary aluminate glasses where the glass forming ability is low. Wilding et al. [9] prepared sticks with composition identical to crystalline yttrium aluminium garnet ($\text{Y}_3\text{Al}_5\text{O}_{12}$, YAG) by sol–gel method, which were then melted in oxygen atmosphere in electric arc. Molten drops were falling through a Pt grid and quenched in water. Other described methods include splat-quenching [10,11] and containerless melting techniques, where the melt is heated by focused laser beam whilst kept in levitation by conical-nozzle or aero-acoustic levitator [12,13]. The flame-spraying synthesis described by Rosenflanz et al. [2] was applied as a suitable method for the preparation of aluminate glasses in the form of microspheres. The crystalline powder precursor was fed into H_2 – O_2 flame and microscopic drops of melt were quenched by spraying with distilled water and collected in a separation tank. The flame synthesis in oxygen–methane flame has been applied by Prnová et al. [14] for the preparation of binary yttrium aluminate glasses with high alumina content. Through

* Corresponding author.

E-mail address: anna.haliakova@tnuni.sk (A. Haliaková).

subsequent hot pressing of prepared microspheres at temperatures up to 1600 °C partially or completely crystalline specimens transparent in IR region and with promising mechanical properties were prepared [15].

In this work the flame synthesis in oxygen–methane flame was applied for the synthesis of binary and ternary glasses in the Al_2O_3 – La_2O_3 system. The lanthanum-based systems have been selected due to the fact that voluminous La^{3+} cations are expected to stabilize amorphous structure in the prepared glasses, thus reducing the tendency to crystallization and improving their glass forming ability in comparison to Al_2O_3 – Y_2O_3 . Small amounts of Er and Nd were added as potentially photo-luminescent additives. Basic physical properties of prepared glasses are reported.

2. Experimental

The compositions of all the prepared systems are summarised in Table 1. Starting powders for flame spraying synthesis were prepared with pure oxides (La_2O_3 – Treibacher Industrie AG, Austria, Al_2O_3 – Taimicron TM DAR, Krahn Chemie GmbH, Germany). Required amount of Al_2O_3 was mixed with the lanthanum nitrate solution, which was prepared by the dissolution of La_2O_3 in concentrated HNO_3 . The mixture was homogenized by ball milling for 2 h. Then, the NH_4OH water solution was added to convert the nitrate to $\text{La}(\text{OH})_3$. The mixture was again homogenized for 4 h to complete the reaction. After drying under infra-red lamp the powder was calcined in an electrically heated furnace at 700 °C for 1 h in air to decompose the nitrates and to convert hydroxides to the respective oxides. Dried powder was crushed and sieved through a 100 μm mesh, and then pre-reacted for 4 h at 1600 °C. The powder was then crushed again, sieved through a 42 μm mesh, and fed to the flame. Nd- and Er-containing precursor powder was prepared in a similar way. Lanthanum oxide was mixed with the requested amounts of Nd_2O_3 or Er_2O_3 and the mixture was dissolved in concentrated HNO_3 . Subsequent procedure was identical to the Al_2O_3 – La_2O_3 system.

Glass microspheres were prepared by flame-spraying technique. The powder precursor was fed into high-temperature CH_4 – O_2 flame ($T \sim 2200$ °C). Molten particles were sprayed

with deionised water to ensure required cooling rate and then collected in sedimentation tank for further separation.

Density of prepared microspheres was determined by liquid pycnometry with hexamethyldisiloxane as the immersion liquid. All measurements were carried out at constant temperature of 20 ± 0.01 °C. Basic information on the morphology of prepared microspheres was obtained by optical microscope (Nikon ECLIPSE ME 600) in transmitted light at 10–50 \times magnification. More detailed information was obtained by SEM (ZEISS EVO 40 scanning electron microscope) at accelerating voltage 20 kV. For the SEM examination the microspheres were fixed at aluminium sample holder using conductive graphite tape and sputtered with gold (Carl-Zeiss SC-7620) to prevent charging during the measurement. IR spectra of powder precursors and microspheres were measured using FTIR spectrometer Nicolet Magna 750 in the wave number range 400–4000 cm^{-1} using standard KBr technique. For spectra treatment and data evaluation, the software OMNIC was used. Differential thermal analysis (DTA-TGA analyser SDT 2960) was used for the determination of glass transition, T_g , onset of crystallisation, T_x , and maximum crystallisation rate temperature, T_c . For the measurements approximately 20 mg of microspheres were placed into Pt crucible and heated in a flow-through atmosphere at 10 °C/min up to 1200 °C.

Phase compositions of powder precursors and prepared microspheres were studied by X-ray diffraction. The STOE RTG powder diffractometer with Co $K\alpha$ radiation with the wavelength 1.78897 Å in the range of 2θ angles 15–85° was used. Subsequently, selected compositions were characterised with the use of high-temperature X-ray diffraction at 850 and 1050 °C. The temperatures were selected on the basis of DTA analysis. The microspheres were fixed on a platinum pad, and the reference X-ray diffraction pattern was recorded at room temperature. Afterwards, the specimen was heated up to 850 °C at a heating rate of 100 °C/min and another diffraction pattern was recorded. The measurement took approximately 60 min. When completed, the temperature was increased up to 1050 °C, and another pattern was recorded. In some cases, one more pattern was recorded after 60 min of isothermal dwell at 1050 °C in order to ensure the completion of crystallization. The data were recorded using a high-temperature X-ray powder diffractometer with Cu $K\alpha$ radiation and the wavelength 1.5405 Å in the 2θ angle range 15–60°. Diffraction patterns were analysed using SW Crystallographica Search-Match box, version 2.1.1.0 (Oxford Cryosystems, Oxford, UK).

3. Results

The results of the microspheres characterisation obtained by optical microscopy are shown in Fig. 1. The micrographs indicate that spherical transparent particles with the diameters changing from 2 μm to 10 μm were prepared. No traces of crystallised (and opaque) or un-melted particles were observed by optical microscopy. Based on these results it can be concluded that the applied flame temperature was sufficient for selected compositions in the Al_2O_3 – La_2O_3 system, with

Table 1
Compositions of prepared systems. The La_2O_3 content represents the difference to 100%. The melting temperature T_m is estimated from the phase diagram La_2O_3 – Al_2O_3 .

Sample	Al_2O_3		Nd_2O_3		Er_2O_3		T_m (°C)
	mol%	wt.%	mol%	wt.%	mol%	wt.%	
A48L52	74.6	47.9	–	–	–	–	1852
A50L50	76.2	50.0	–	–	–	–	1815
A54L46	79.0	54.1	–	–	–	–	1835
A58L42	81.8	58.4	–	–	–	–	1875
A62L38	83.8	61.8	–	–	–	–	1890
A68L32	86.9	67.5	–	–	–	–	1925
A50L50Nd	75.7	48.9	1.0	2.1	–	–	–
A50L50Er	75.7	48.8	–	–	1.0	2.4	–

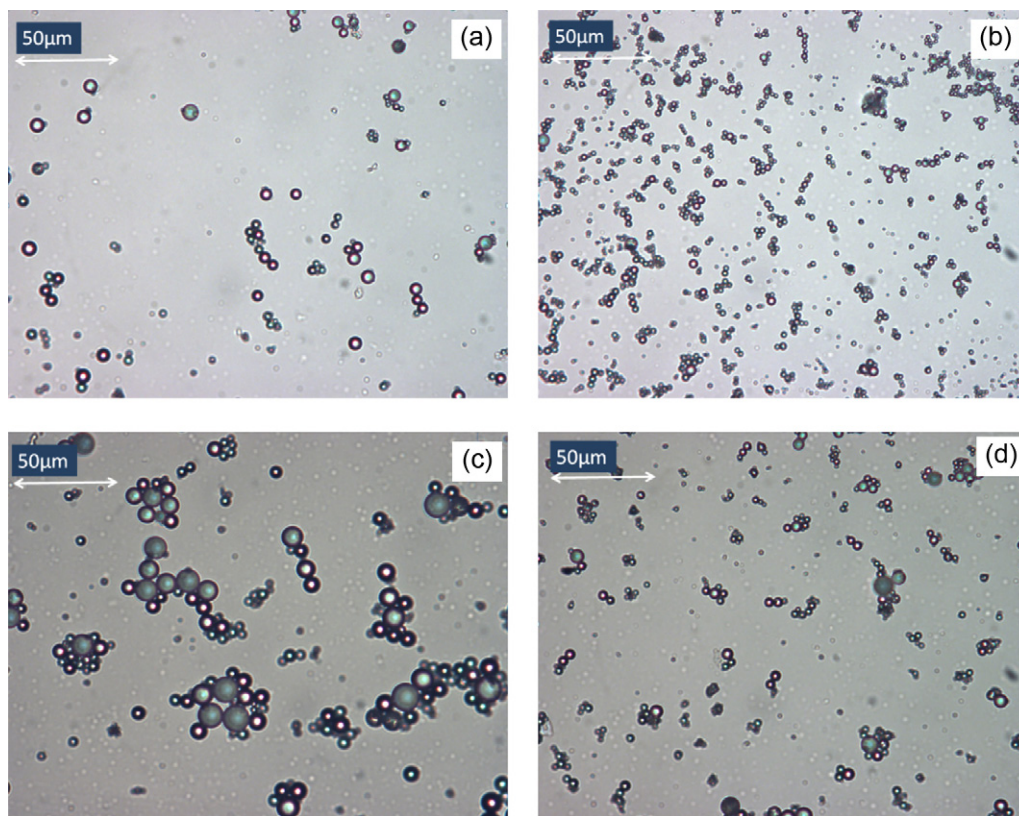


Fig. 1. The optical microscopy photographs of prepared microspheres: (a) A58L42, (b) A68L32, (c) A50L50Er, and (d) A50L50Nd.

melting temperatures ranging between 1815 and 1925 °C, as estimated from the phase diagram.

More detailed examination of prepared micro-beads was carried out by scanning electron microscopy (Fig. 2). Major part of all the specimens contained only regular spherical particles with smooth surfaces without any traces of crystallization. However, partly or totally crystalline microspheres appeared sporadically. Such features were present especially in particles with diameters $>10\text{ }\mu\text{m}$ due to the insufficient cooling rate in microspheres with low thermal conductivity. With growing alumina content the fraction of partly crystalline microspheres is increasing. This effect is explained by higher melting temperatures, as well as by growing tendency to crystallization with increasing Al_2O_3 content.

Results of density measurements of microspheres of various compositions are given in Fig. 3. The values ranged in the interval from 3.85 g cm^{-3} (sample A68L32 containing 86.9 mol% Al_2O_3) up to 4.77 g cm^{-3} (sample A48L52 containing 74.6 mol% Al_2O_3). The density of prepared microspheres decreases with increasing Al_2O_3 content.

DTA records of microspheres are presented in Fig. 4. In most cases, the glass transition temperature T_g of prepared glasses could not be identified from the DTA records. The only exception is the composition A50L50 where an insignificant maximum is visible on the DTA curve at temperature about 700 °C, directly followed by extensive and clear exothermic effect. The former can be, with some caution, interpreted as the T_g . Based on this, we can assume that the glass transition

temperatures of all the prepared glasses will be close to this temperature, also with regard to their expected structural similarity. Exothermic maxima corresponding to the temperature of maximum crystallisation rate T_c were observed at temperatures from 918 °C (compositions A54L46 and A58L42) up to 940 °C (compositions A48L52–A68L32). The crystallization proceeds in most prepared systems in two stages, as indicated by the presence of two exothermic maxima in DTA records of samples with the alumina content exceeding 54 wt.% (compositions A54L46–A68L42), with the first maximum appearing at 918 °C and the second one at 940 °C. In samples with lower alumina content these combine creating one broad exothermic peak with maximum at 930 °C observed for the compositions A48L52 and A50L50. The presence of another exothermic effect can be observed in the A50L50 system in temperature interval 1250–1300 °C. The origin of this maximum is not clear at present.

The results of X-ray diffraction phase analysis are summarized in Fig. 5. Precursor powders were crystalline although in some compositions (A50L50, A62L38, A68L32) the diffraction intensities were extremely low (Fig. 5a). Two crystalline phases were identified in all powders, regardless of composition, especially lanthanum–aluminium perovskite LaAlO_3 , and in smaller volume fractions $\text{LaAl}_{11}\text{O}_{18}$ (sometimes also referred to as $\beta\text{-La-Al}_2\text{O}_3$). Prepared microspheres (Fig. 5b) although mostly amorphous, all contained small volume fractions of crystalline phases, except of the A58L42 system that appears XRD amorphous. The largest fraction of

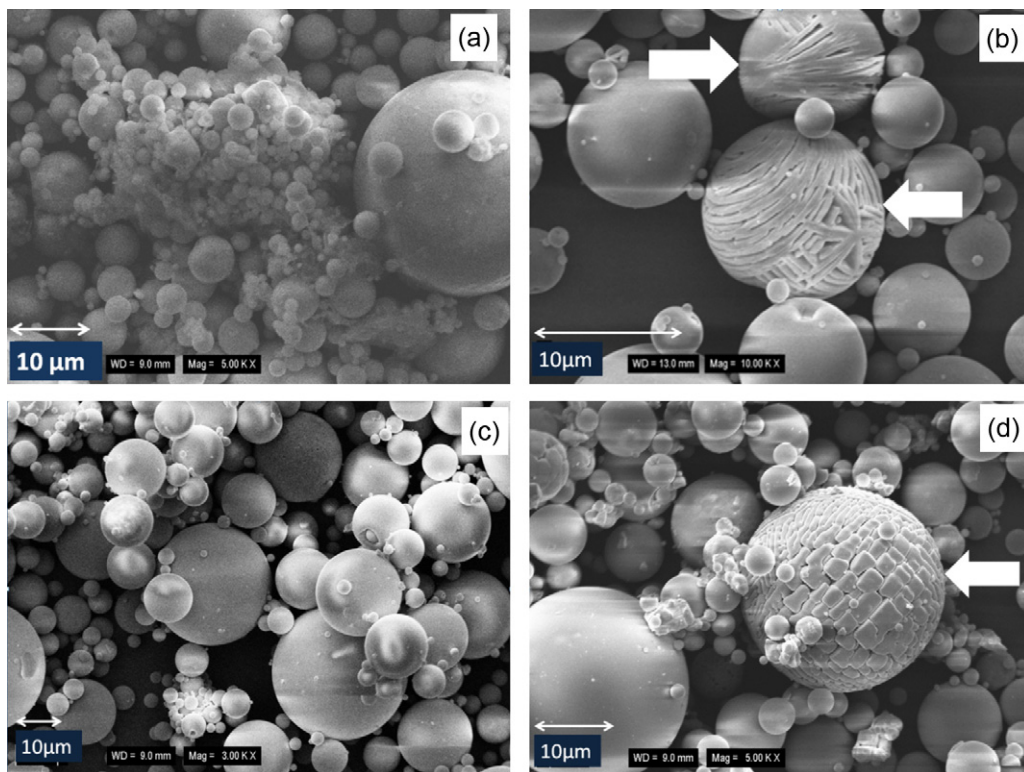


Fig. 2. The SEM micrographs of prepared microspheres: (a) A58L42, (b) A68L32, (c) A50L50Er and (d) A50L50Nd. Fully or partially crystalline microspheres are marked by arrows.

crystalline phases was detected in A54L46. However, the intensities of diffraction peaks were very low in all records, indicating highly amorphous character, and very small volume fraction of crystalline phases, in all prepared microspheres. Unlike the precursor powders, only one crystalline phase, lanthanum–aluminium perovskite LaAlO_3 , was identified in the microspheres. The only exception is the composition with the highest Al_2O_3 content, A68L32, where traces of the $\text{LaAl}_{11}\text{O}_{18}$ phase could be also identified. The Er and Nd doping had no observable influence on phase composition: neodymium doped

system contained small amounts of LaAlO_3 phase whilst erbium doped samples were X-ray amorphous.

The results of high-temperature X-ray diffraction are summarized in Fig. 6. To define crystallization process we selected two compositions: A50L50 eutectic composition where we could expect the lowest tendency to crystallization and A68L32 composition with the highest Al_2O_3 content

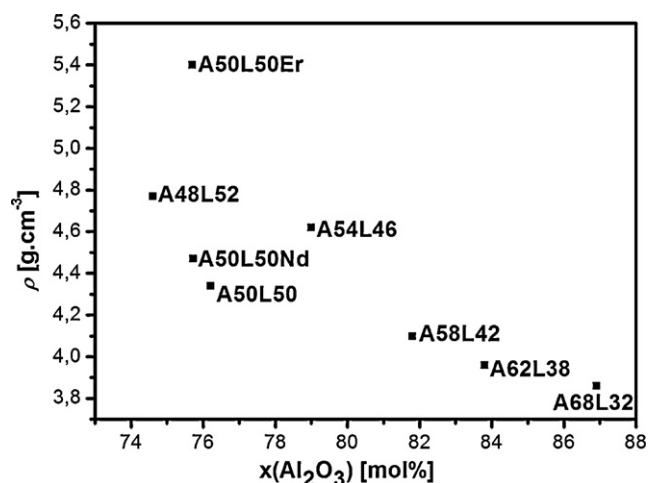


Fig. 3. The dependence of the density of microspheres on their compositions.

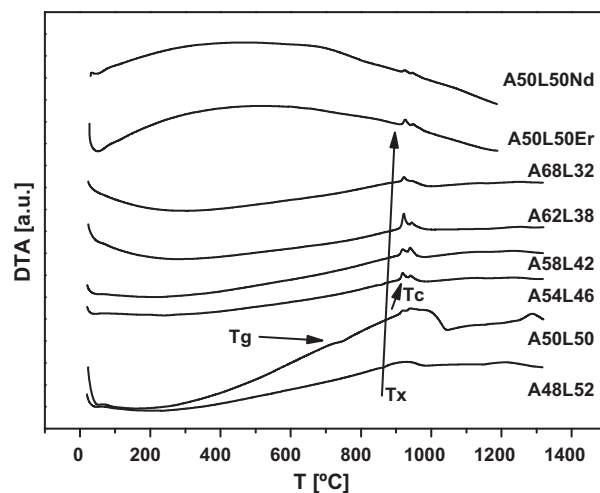


Fig. 4. The results of DTA analysis of prepared microspheres. T_g , T_x , and T_c stand for glass transition temperature, onset of crystallization temperature, and the temperature of maximum crystallization rate, respectively. The T_x and T_c are slightly shifted to higher temperatures, as highlighted by the arrow.

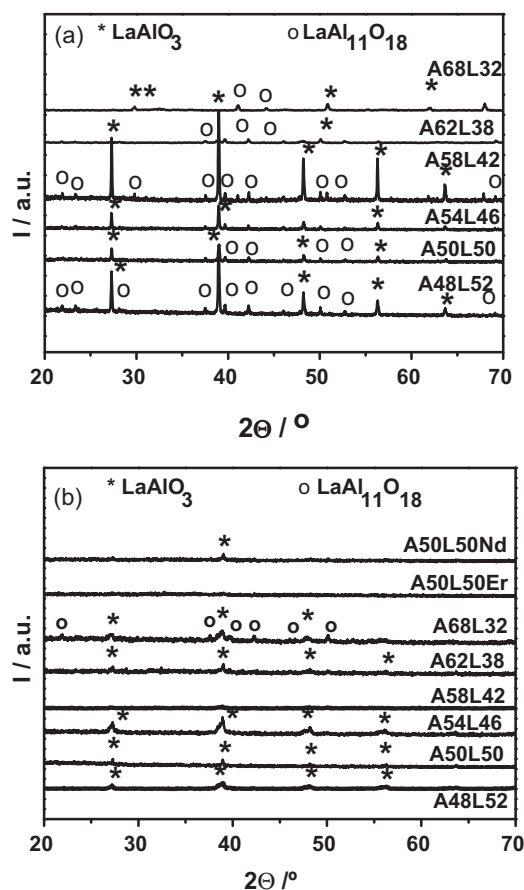


Fig. 5. The X-ray diffraction patterns of prepared precursor powders (a) and microspheres (b).

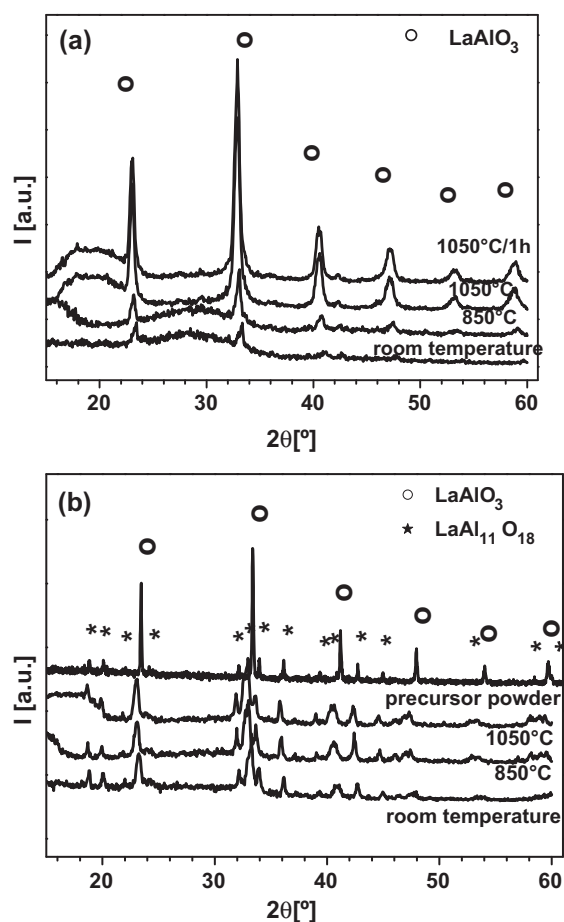


Fig. 6. The results of high-temperature X-ray diffraction phase analysis of prepared systems (a) A50L50 and (b) A68L32.

where, on the contrary, high tendency to crystallization was expected. As seen in Fig. 6, with growing temperature the diffraction peaks are systematically shifted to lower 2θ values due to the change of lattice parameters resulting from thermal expansion of crystal lattice. The peaks are relatively broad, which is most likely because of the presence of small sized crystals, at the level of several tens of nm. Crystallization of a single phase, lanthanum–aluminium perovskite, LaAlO_3 , takes place at the eutectic composition A50L50 (Fig. 6a). Even at the temperature as low as 850 °C certain increase of diffraction peaks intensities in comparison to the room temperature measurement could be observed. This increase was more pronounced during measurements at the temperature of 1050 °C. Subsequent isothermal heating (1 h at 1050 °C) did not bring any visible change of diffraction intensities. Based on this fact we concluded that the crystallization of the specimen was completed. Two crystalline phases were identified in the sample A68L32 already at room temperature (Fig. 6b). LaAlO_3 perovskite phase was present as in the case of the composition A50L50, accompanied by smaller amount of $\text{LaAl}_{11}\text{O}_{18}$ phase. Such phase composition agrees with the composition expected from the phase diagram of the studied system. However, during the high-temperature experiment no visible change in

diffraction intensities was observed, even at 1050 °C. This indicates high thermal stability and high resistance to crystallization of the composition A68L32.

IR spectroscopy revealed that all the studied compositions, both the precursor powders and microspheres were IR transparent in the wavenumber interval from 1300 to 4000 cm^{-1} . As no vibration bands were detected in the IR spectra in this interval, only parts of the spectra in the interval between 400 and 1500 cm^{-1} are shown in Fig. 7. Vibration bands in all the prepared systems were poorly resolved, and apart from some exceptions, they contain no clearly defined sharp peaks but rather wide bands that indicate highly amorphous character of prepared microspheres with high measure of structure disorder and large interval of vibration energies. As seen from the comparison of the spectra of individual systems, the highest fraction of amorphous phase can be expected for the composition A50L50—the eutectic with the lowest melting temperature, and in the A58L42 sample. Spectra of these specimens consist of a single wide absorption band in the wave-number interval from 400 to 1300 cm^{-1} . For other compositions with lower Al_2O_3 content (A48L52 and A54L46) it is possible to distinguish two wide bands in the intervals 400–600 cm^{-1} , and 600–800 cm^{-1} , with maxima at 470 and 660 cm^{-1} , respectively. Absorption maxima of samples with

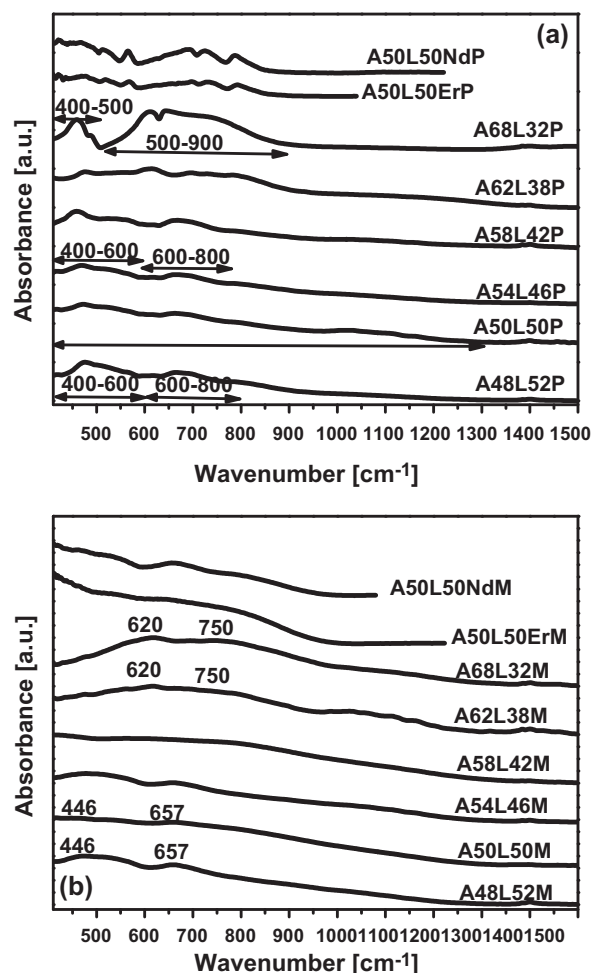


Fig. 7. The IR spectra of precursor powders (a) and prepared microspheres (b). The numbers represent the maxima of vibration bands.

higher Al₂O₃ contents (A62L38 and A68L32) were shifted to higher wavenumber values, i.e. to 620 and 750 cm⁻¹.

4. Discussion

Measured densities of the prepared glasses decrease monotonously with increasing Al₂O₃ content. Regarding the similarities observed in IR spectra, as well as the results of X-ray diffraction the trend can be interpreted as the combination of reduced content of the component with high molar weight and density, i.e. La₂O₃, accompanied by structure change of prepared glasses. The only exception is the composition A54L46 (79.0 mol% Al₂O₃) whose density 4.62 g cm⁻³ is significantly higher than expected on the basis of its composition. However, the deviation is due to relatively high content of LaAlO₃ crystalline phase in comparison to other compositions, as shown by the results of X-ray diffraction.

These assumptions are also supported by the IR spectroscopy results. To our knowledge, the Al₂O₃–La₂O₃ system was not studied extensively by IR spectroscopy so far, and only limited information is therefore available in the published literature. Exact interpretation of measured spectra based on

literature data is, therefore, not possible, and can only be carried out with reference to IR spectra of other rare earth aluminates, such as Al₂O₃–Y₂O₃. In these systems, gradual disappearance of vibration bands at 431 and 474 cm⁻¹ corresponding to Al–O vibrations in tetrahedral co-ordination in YAG structure [16–21], and increase in the intensity of bands at 490 and 592 cm⁻¹ corresponding to Al–O vibrations of octahedrally coordinated aluminium atoms characteristic for α-Al₂O₃ was observed with increasing alumina content [22]. Similarly, the presence of a band in the wavenumber ranging from 1000 to 1200 cm⁻¹ can be attributed to Al–O vibrations in structures with octahedrally coordinated aluminium atoms. The results indicate gradual increase of the coordination number of aluminium atoms in the glass structure from 4 to 6 that could be observed in yttrium–aluminium glasses with higher Al₂O₃ content [22]. It is a matter of discussion whether the vibration maxima changes observed in the samples with high alumina contents in this work can be attributed to such a change of aluminium atom coordination, especially due to the fact that garnet structures of the composition La₃Al₅O₁₂ were not described in the literature. However, by more detailed study of the spectrum of the sample A50L50 we observed two weak absorption maxima at 446 and 657 cm⁻¹ within the major absorption band 400–1300 cm⁻¹ that were observed in aluminates with perovskite structures [23]. These could be also identified as weak maxima at 470 and 660 cm⁻¹ of broad vibration bands in the A48L52 and A54L46 compositions. Their gradual disappearance with increasing content of Al₂O₃ in glasses, as well as the shift of absorption maxima to higher wavenumbers, can be caused by the change of coordination number of aluminium atom from 4 to 6. These conclusions are supported also by the results of X-ray diffraction, which revealed crystallization of LaAl₁₁O₁₈ (also described in the literature as La-β-Al₂O₃ [24]) in the A68L32 system.

The presence of small amount of LaAlO₃ perovskite as the only crystalline phase was confirmed in the prepared microspheres in majority of studied compositions. With increasing temperature the intensities of diffraction peaks of the perovskite phase increased at temperatures as low as 850 °C, and the crystallization was practically completed after 1 h of isothermal dwell at 1050 °C, with the perovskite phase as the only crystalline phase present. In the sample A68L32 with the highest Al₂O₃ content two phases were present even at room temperature: LaAlO₃ perovskite, together with LaAl₁₁O₁₈, which indicates the presence of structural units with octahedral co-ordination of aluminium atoms in amorphous aluminate network. It is interesting that diffraction intensity during high temperature X-ray experiments remains unchanged regardless of the temperature, and even after 1 h isothermal experiment at 1050 °C, no observable change of phase composition takes place. Such result is the indication of relatively high thermal stability of the A68L32 system. More detailed study of such behaviour will be the subject of further research. Some hints are provided by the work of Costa and Muccillo [24], who reported that the temperature up to 1500 °C was required for complete synthesis and crystallization of La-β-Al₂O₃ (LaAl₁₁O₁₈) phase.

5. Conclusions

The work describes preparation of binary aluminate glasses in the $\text{La}_2\text{O}_3\text{--Al}_2\text{O}_3$ system with high alumina content (up to 86.9 mol%) by flame synthesis in the form of microspheres, and of ternary glasses containing 1 mol% of potentially photoluminescent additives Nd_2O_3 or Er_2O_3 . Prepared microspheres are mainly amorphous, with only small fraction of crystalline aluminates LaAlO_3 (perovskite) and $\text{LaAl}_{11}\text{O}_{18}$ ($\text{La-}\beta\text{-Al}_2\text{O}_3$). The latter was detected only in compositions with the highest Al_2O_3 content (86.9 mol%). Prepared microspheres were IR transparent in the wavenumber range $1300\text{--}4000\text{ cm}^{-1}$. IR spectra in the wavenumber range from 400 to 1300 cm^{-1} indicate changes in the structure of prepared glasses with increasing alumina content, with gradual change of the aluminium coordination number from 4, characteristic for LaAlO_3 , to 6 typical for $\text{La-}\beta\text{-Al}_2\text{O}_3$ ($\text{LaAl}_{11}\text{O}_{12}$) or $\alpha\text{-Al}_2\text{O}_3$. Fully crystalline LaAlO_3 could be prepared by the crystallization of A50L50 microspheres at 1050°C . No significant influence of Er_2O_3 and Nd_2O_3 doping on the structure, and phase composition of prepared glasses was observed.

Acknowledgements

The financial support of this work by the grant VEGA 2/0076/10, and the APVV grant LPP 0133-09 is gratefully acknowledged. This publication was created in the frame of the project “Centre of excellence for ceramics, glass, and silicate materials” ITMS code 26220120056, based on the Operational Program Research and Development funded from the European Regional Development Fund.

References

- [1] J.R. Berchmans, S. Angappan, A. Visuvasam, K.B.R. Kumar, Preparation and characterization of LaAlO_3 , *Materials Chemistry and Physics* 109 (2008) 113–118.
- [2] A. Rosenflanz, M. Frey, B. Endres, T. Anderson, E. Richards, C. Schardt, Bulk glasses and ultrahard nanoceramics based on alumina and rare-earth oxides, *Nature* 430 (2004) 761–764.
- [3] P.F. McMillan, W.T. Petuskey, B. Coté, D. Massiot, C. Landron, J.P. Coutures, A structural investigation of $\text{CaO--Al}_2\text{O}_3$ glasses via ^{27}Al MAS-NMR, *Journal of Non-Crystalline Solids* 195 (1996) 261–271.
- [4] J. Johnson, R. Weber, M. Grimsditch, Thermal and mechanical properties of rare earth aluminate optical glasses, *Journal of Non-Crystalline Solids* 351 (2005) 650–655.
- [5] J.K.R. Weber, J.J. Celtem, B. Cho, P.C. Nordine, Glass fibres of pure and erbium- or neodymium-doped yttria–alumina compositions, *Nature* 393 (1998) 769–771.
- [6] C.J. Benmore, J.K.R. Weber, J.E. Siewenie, K.J. Hiera, Structure of Nd-doped glasses measured by isotopic substitution in neutron diffraction, *Applied Physics Letters* 83 (2003) 4954–4956.
- [7] A. Aronne, S. Esposito, P. Pernice, FTIR and DTA study of lanthanum aluminosilicates glasses, *Materials Chemistry and Physics* 51 (1997) 163–168.
- [8] M. Karabulut, E. Metwalli, R.K. Brow, Properties and structure of lanthanum aluminophosphate glasses, *Journal of Non-Crystalline Solids* 283 (2001) 211–219.
- [9] M.C. Wilding, C.J. Benmore, P.F. McMillan, A neutron diffraction study of yttrium- and lanthanum-aluminate glasses, *Journal of Non-Crystalline Solids* 297 (2002) 143–155.
- [10] F. Flunder, B.S. Mitchell, Infrared studies of processing effects in calcium aluminate glasses, *Journal of Non-Crystalline Solids* 224 (1998) 184–190.
- [11] A.Y. Haeri, C.T. Ho, R. Weber, J. Diefenbacher, P.F. McMillan, Elastic properties of aluminate glasses via Brillouin spectroscopy, *Journal of Non-Crystalline Solids* 241 (1998) 200–203.
- [12] J.K.R. Weber, J.H. Abadie, A.D. Hixson, P.C. Nordine, G.A. Jerman, T.E. Mitchell, Glass formation and polymorphism in rare-earth oxide–aluminum oxide compositions, *Journal of the American Ceramic Society* 83 (2000) 1868–1872.
- [13] J.K.R. Weber, J.G. Abadie, T.S. Key, K. Hiera, P.C. Nordine, Synthesis and optical properties of rare earth–aluminum oxide glasses, *Journal of the American Ceramic Society* 85 (2002) 1309–1311.
- [14] A. Prnova, R. Karell, D. Galusek, The preparation of binary $\text{Al}_2\text{O}_3\text{--Y}_2\text{O}_3$ glass microspheres by flame synthesis from powder oxide precursors, *Ceramics-Silikaty* 52 (2008) 109–114.
- [15] A. Prnová, D. Galusek, M. Hnatko, J. Kozánková, I. Vávra, Composites with eutectic microstructure by hot pressing of $\text{Al}_2\text{O}_3\text{--Y}_2\text{O}_3$ glass microspheres, *Ceramics-Silikaty* 55 (2011) 208–213.
- [16] D. Boyer, G. Bertrand-Chadeyron, R. Mahiou, Structural and optical characterizations of YAG:Eu^{3+} elaborated by the sol–gel process, *Optical Materials* 26 (2004) 101–105.
- [17] S. Tsao, Y.-P. Fu, C.-T. Hu, Preparation of $\text{Y}_3\text{Al}_5\text{O}_{12}:\text{Sm}$ powders by microwave-induced combustion process and their luminescent properties, *Journal of Alloys Compound* 419 (2006) 197–200.
- [18] S. Tsao, Y.-P. Fu, C.-T. Hu, Preparation of $\text{Y}_3\text{Al}_5\text{O}_{12}:\text{Cr}$ powders by microwave-induced combustion process and their luminescent properties, *Journal of Alloys Compound* 395 (2005) 227–230.
- [19] S. Mathur, H. Shen, A. Lelekaite, A. Beganskiene, A. Kareiva, Low-temperature synthesis and characterization of yttrium–gallium garnet $\text{Y}_3\text{Ga}_5\text{O}_{12}$ (YGG), *Materials Research Bulletin* 40 (2005) 439–446.
- [20] A. Lelekaite, A. Kareiva, H. Bettentrup, T. Ustel, H.-J. Meyer, Sol–gel preparation and characterization of codoped yttrium aluminium garnet powders, *Zeitschrift für Anorganische und Allgemeine Chemie* 631 (2005) 2987–2993.
- [21] Y.H. Zhou, J. Lin, S.B. Wang, J.H. Zhang, Preparation of $\text{Y}_3\text{Al}_5\text{O}_{12}:\text{Eu}$ phosphors by citric gel method and their luminescent properties, *Optical Materials* 20 (2002) 13–20.
- [22] R.A. Niquist, R.O. Kagel, *Infrared Spectra of Inorganic Compounds*, Academic Press, New York and London, 1971.
- [23] E. Garskaite, N. Dubnikova, A. Katelnikovas, J. Pinkas, A. Kareiva, Syntheses and characterisation of $\text{Gd}_3\text{Al}_5\text{O}_{12}$ and $\text{La}_3\text{Al}_5\text{O}_{12}$ garnets, *Collection of Czechoslovak Chemical Communications* 72 (2007) 321–333.
- [24] G.C.C. Costa, R. Muccillo, Synthesis of lanthanum beta-alumina powders by the polymeric precursor technique, *Ceramics International* 34 (2008) 1703–1707.